DOI: 10.13009/EUCASS2022-6151
9TH EUROPEAN CONFERENCE FOR AERONAUTICS AND SPACE SCIENCES (EUCASS)

Experimental study on the low-pressure turbine wake interaction and development in the turbine rear structure

Valentin Vikhorev, Isak Jonsson*, Mikhail Tokarev* and Valery Chernoray**
**Chalmers University of Technology, Department of Mechanics and Maritime sciences*
Gothenburg, SE-41296, Sweden
valvik@chalmers.se

Abstract

The aerodynamic characteristics of advanced turbine rear structures (TRSs) could be affected by the interaction between unsteady flow developed from low-pressure turbine (LPT) and outlet guide vanes (OGVs). Consequently, analyzing the details of the interactions between the rotor wakes, stator wakes and OGVs is essential to enhance the aerodynamic efficiency of the modern TRS. This paper presents time resolved flow field measurements in the TRS at engine representative flow conditions. Experiments were performed in an annular large-scale 1.5 stage turbine facility at Chalmers University of Technology, Laboratory of Fluid and Thermal Sciences. The facility provides engine-realistic boundary conditions for the TRS and experimental data were acquired using 5-hole and 7-hole probes (5HP and 7HP), hot-wire anemometry (HW) and Particle Image Velocimetry (PIV). The PIV and HW measurements were conducted for the first time to enhance the understanding of unsteady flow phenomena and to investigate the development of TRS inflow structures. The observed unsteady interaction mechanism between the rotor wakes, stator wakes and OGV is of prime interest and investigated in detail. The breakdown of rotor and stator wakes through the TRS are documented and the OGV wake is analysed in detail by PIV.

1. Introduction

Engine fuel efficiency and weight optimisation are high priority goals in all aero-engine designs. The introduction of geared turbofan engines (GTFs) was a major leap forward in jet engine technology. A gear system separates the fan and the low-pressure turbine (LPT) and allows the LPT and fan to rotate at optimal speeds. This feature increases propulsive efficiency and leads to noise reduction. Moreover, the lighter weight produced by fewer components provides further fuel savings and CO_2 reduction.

Maintaining the flow exits LPT in the axial state is crucial to maximise the engine thrust. Therefore, an aeroengine has a turbine rear structure (TRS) that needs to serve a structural function connecting the engine core to the aircraft wing and straightening the flow through outlet guide vanes (OGVs), see Fig. 1. Since the engine mounting relies on the TRS, the structural integrity of TRS is vital. Therefore, the OGVs are large, and study of the flow aerodynamics is an essential part of the development of a new TRS design.

The inflow to the TRS is highly dynamic and unsteady due to the relative motion of blade surfaces in the LPT stage. The rotation causes the potential flow field and rotor secondary flows interact periodically [1, 2]. Moreover, the development of boundary layers on nozzle guide vanes (NGV) and rotor blades within LPT leads to the formation of wakes and secondary flows involved in the interaction process. Many research works discussed wake characteristics and the secondary flow evolution in the linear and annular cascades of airfoils. Near and far wake characteristics of a cascade airfoils were investigated in detail by Raj and Lakshminarayana [3]. They provided a complete wake analysis showing the asymmetrical nature of the wake and slower decay of wakes compared to flat plate and cylinder cases. The secondary or endwall flows and their development in a cascade of turbine blades or vanes are well studied by many researchers [4−8] and summarized by Langston [9]. The evolution of vortices and wakes through downstream blade rows leads to the two main type of stator-rotor interaction: “stator wake-rotor blade” and “stator secondary flows-rotor blade” (except for interactions related to endwall regions). For the LPT, the first type of interaction is dominant due to the low Reynolds number and higher blade height. The incoming wakes from upstream cascades interacting with the boundary layer of stator vanes could trigger a laminar-turbulent transition. It increases the capability to resist against adverse pressure gradient, consequently delaying boundary layer separation and reducing the strength of secondary flows. Therefore, interactions between different rows of blades are mainly due to the “stator wake-rotor blade” interaction. It is shown that wake induced transition significantly influences the boundary layer behaviour of blades under typical LPT operating conditions [10, 11]. A complete review of mechanisms related to the unsteady wake-blade interaction can be found in Hodson [12]. However, with numerous papers related to the stator-rotor

DOI: 10.13009/EUCASS2022-6151

interaction, there has been no discussion in the literature about the LPT wake development and interaction with the downstream OGVs.

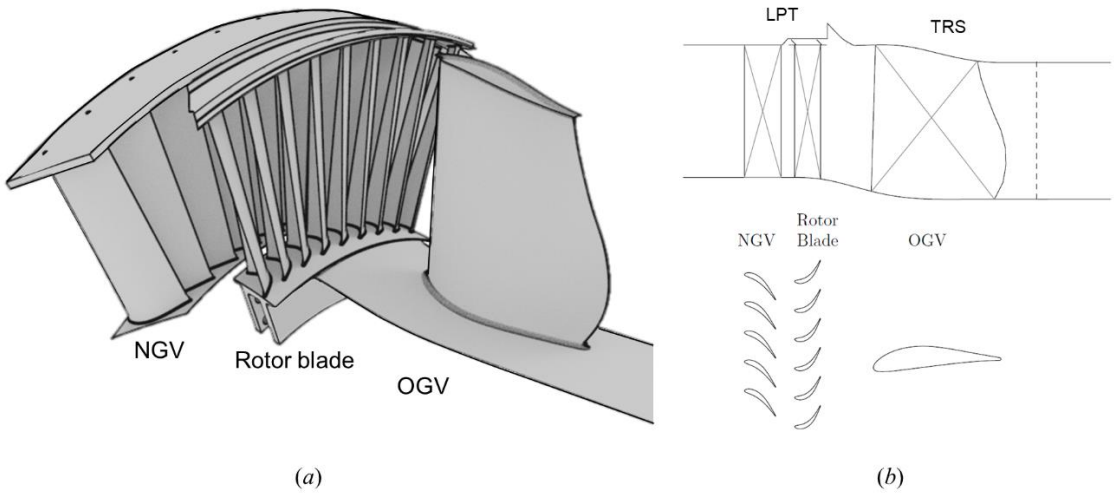

Figure 1: The schematic of LPT and TRS: (*a*) isometric view (*b*) meridional view with midspan profiles.

The main aerodynamic purpose of OGVs is to remove the exit swirl from the LPT's last rotor stage. As mentioned above, the interaction of OGVs with LPT wakes complicates the flow further and leads to pressure losses generated in the endwall and OGV boundary layers. The low-momentum flow close to the hub is very sensitive, requiring proper aero-design due to the (1) skewed velocity profile of the endwall boundary layer in combination with (2) acting circumferential and radial pressure gradients with corresponding induced cross flow, and (3) adverse pressure gradient caused by the diffusion of the passage. For large mass flow rate conditions or low loaded vane, the development of the boundary layer in the hub corner does not lead to a corner separation. However, increasing the inlet swirl angle (more loaded vane) or lowering the mass flow rate can significantly affect the hub corner region and introduce three-dimensional corner separation with additional losses. Moreover, the OGV boundary layer on the suction side is affected by the radial fluid migration and streamwise adverse pressure gradient. As a result, a separation bubble can occur. However, based on flow visualisations performed for investigated configuration in the on-design case, the formation of the separation bubble was usually followed by laminar-turbulent transition and turbulent reattachment without notable contribution to pressure losses [13]. The laminar-turbulent transition, heat transfer and surface roughness of OGVs in TRS were investigated by Jonsson et al. [14−16] and Deshpande et al. [17]. More detailed experimental and numerical investigation of the TRS in an engine-realistic environment can be found in [18, 19].

The unsteady flow effects, that originate due to the interaction between wakes and developed boundary layers from endwalls and OGVs can have a major influence on the flow field in the TRS and contribute to a large extent to the generation and redistribution of pressure losses. Therefore, an accurate wake analysis is crucial when predicting TRS performance. To the author's knowledge no research papers have been published describing the development of LPT wakes in TRS. Therefore, the aim of the paper is to experimentally investigate the interaction and propagation of TRS inflow structures within TRS. Results from the first Particle Image Velocimetry (PIV) and hot-wire anemometry (HW) experimental campaigns are presented in this paper with aim to extract additional information about the complex flow features.

2. Experimental setup

2.1 Experimental facility and test conditions

The measurements were performed in a low speed 1.5 stage large-scale LPT-OGV facility at Chalmers University of Technology, Sweden. Figure 2 shows the schematic view of the facility. The rig consists of a centrifugal fan, a semi-closed loop duct system with diffusers and corner blades needed to guide the flow, a heat exchanger to establish stable temperature, a settling chamber with turbulent grids and honeycombs to obtain high flow uniformity, a contraction, a turbine stage to provide engine representative LPT operating conditions and a modular TRS that can be switched to test different configurations. The turbine's rotational speed is controlled by a hydraulic brake system that allows to set the flow coefficient φ defined as ratio between tangential speed of turbine and axial flow velocity.

DOI: 10.13009/EUCASS2022-6151

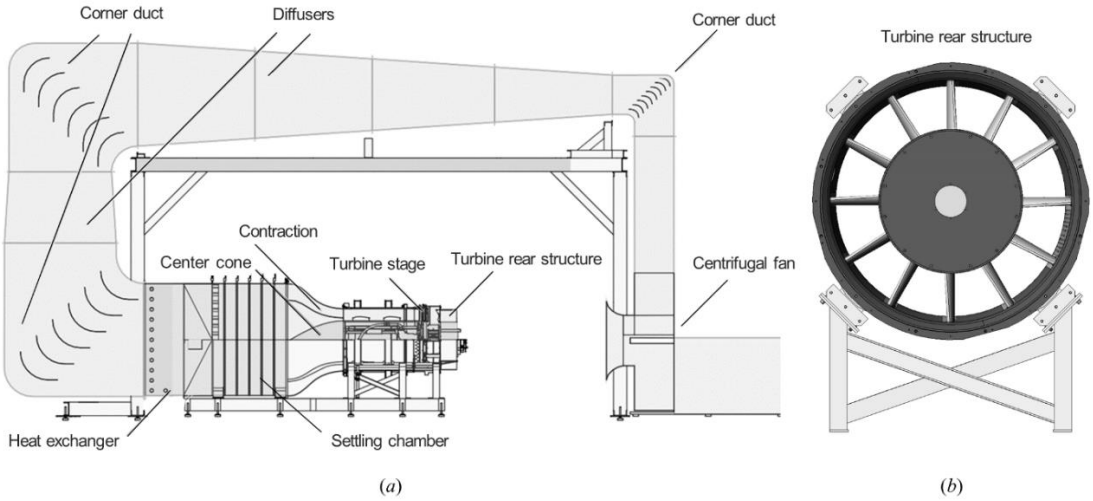

Figure 2: The schematic view of (*a*) LPT-OGV rig and (*b*) TRS.

The Reynolds number *Re* is another operating parameter based on the axial flow velocity and TRS channel height at the inlet. The LPT stage has 60 stator vanes and 72 rotor blades. The rotor blades are shrouded, and the tip flow leakage is representative of aero engines in terms of the mass flow and the ratio between the core flow and the leakage flow. The aero surfaces of rotor blades and stator vanes in the LPT and TRS are designed by GKN Aerospace Sweden while the instrumentation and mechanical design were made by Chalmers University of Technology. However, it shall be noted that the aero surfaces have been developed solely for the experimental rig and are not related to any GKN Aerospace product characteristics. The specifications of the stator and rotor cascades with more detailed description of the rig can be found in [20]. Investigated TRS configuration has 12 OGVs mounted with 30-degree spacing as shown in Fig. 2, (*b*).

Tests were done at the on-design condition corresponding to flow coefficient equals 0.622 and Reynolds number of 235,000. The flow coefficient corresponds to circumferentially averaged LPT exit swirl angle of 17 degrees. The inlet turbulence intensity in the rig is 5% [14]. The flow in this experiment is incompressible because the Mach number based on the exit conditions is well below 0.1.

2.2 Experimental techniques

Figure 3 depicts an isometric view of the TRS with schematically shown experimental instrumentation used throughout this research.

Steady-state measurements were done using 5-hole and 7-hole pressure probes (5HP and 7HP) located upstream and downstream OGV. The data are presented in the form of mean velocity values converted from dynamic pressure. The reference total and static pressure values were measured by a Prandtl tube located between OGVs at 0.7 chord distance from the leading edge in the bulk flow region.

Unsteady velocity measurements of streamwise velocity component *u* were done by HW probe using the same slot used for the 7HP downstream measurements. The HW probe employed in the present investigation was equipped with a tungsten wire of 5 µm diameter and 1 mm in length and operated in the constant temperature mode by a Dantec CTA 56C17 anemometer. The sampling frequency was 100 kHz to satisfy the Nyquist criterion and the sampling time was 0.2 s at each point. The hot wire was calibrated in a jet generated by the calibration facility described in [21]. Measured voltage data were converted into the velocity data using a calibration curve and then the ensemble averaged over 10 blocks. Data are presented in the form of standard deviation of ensemble averaged velocity and perturbation velocity which is defined as the difference between the ensemble-averaged and time-averaged velocities:

$$u_{\mathrm{p}} = u_{\mathrm{aver}} - u_{\mathrm{mean}} \tag{1}$$

Moving upstream and downstream probes (marked with red and blue colors in Fig. 3) was carried out utilising separate traverse systems. For HW measurements, the downstream probe was capable of axial motion to cover the volume between OGVs. Radial and axial positioning of probes were done with an accuracy of 0.075 mm, while for the circumferential positioning the accuracy was 0.01 deg. Calibration of the HW probe was performed in the free stream with a Prandtl tube positioned in close proximity to the probe.

DOI: 10.13009/EUCASS2022-6151

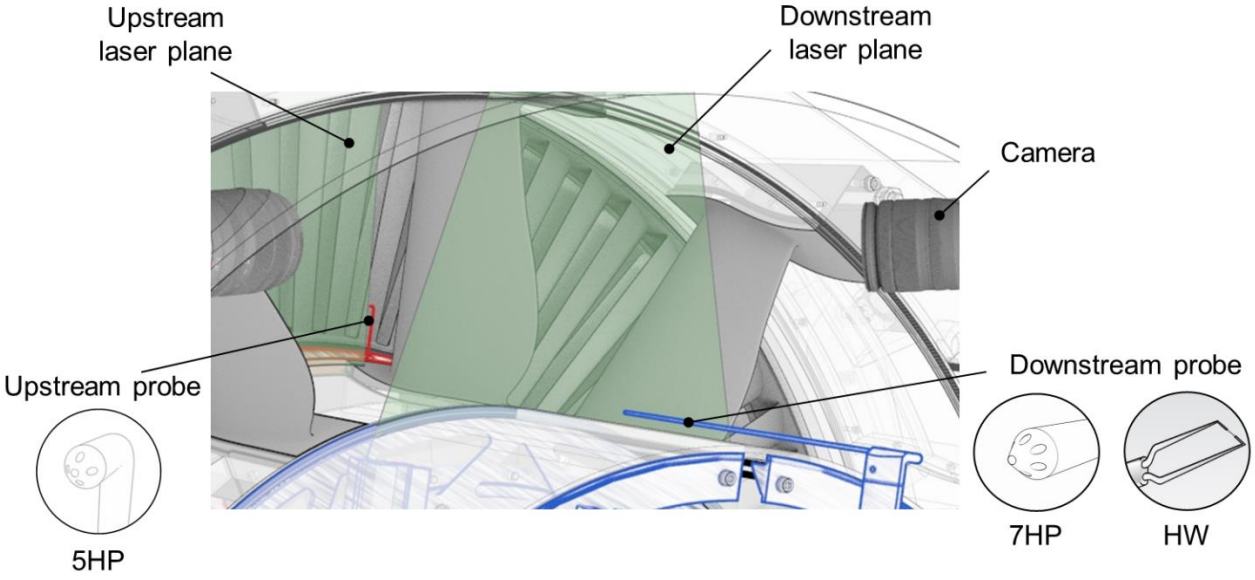

Figure 3: Isometric view of the test section with probes and laser planes located upstream and downstream OGVs for total pressure, HW and PIV measurements.

Two CCD cameras did stereo PIV acquisition at the upstream plane, ImagerProX 4M from LaVision GmbH with 2048 × 2048 pixel resolution, and at the downstream plane with two SpeedSenseM340 CMOS Dantec cameras (see Fig. 3) with 2560 × 1600 pixel resolution. Cameras were equipped with 105-mm f/2.8 lenses from Sigma. Upstream cameras were sampled at 2-3 Hz triggered with the turbine RPM and downstream cameras at 400 Hz which were non-synchronized with the turbine RPM. The laser illumination was provided through transparent windows implemented in the shroud at upstream and downstream laser planes shown in Fig. 3. Quantel EverGreen Nd:YAG laser with pulse energy of 200 mJ did upstream illumination and Litron LDY304 Nd:YLF laser with 20 mJ was used for downstream illumination. Seeding was done on demand by a glycol-based fluid generator at the inlet of the driving fan. The software used to acquire, and process data was Dantec's Dynamic Studio 2016 and LaVision's DaVis 8. The original images were pre-processed by subtracting the minimum brightness over ensemble images to reduce the contribution of background noise. A mask was applied to the images, removing areas with a low signal level and solid boundaries. Multipass stereo PIV processing was performed with a final interrogation area size of 48 × 48 pixels with a 75% overlap for the upstream plane and 16 × 16 pixels with 50% overlap for the downstream plane, adapting to the seeding particle density and image quality. The final post-processing of data was performed in the Matlab software package.

3. Results and discussions

The measurement results of the steady and time-resolved flow field are shown in this section. All measurements in the present investigation were performed at on-design conditions at the inlet flow coefficient $\varphi = 0.622$ and Reynolds number Re = 235,000. The first subsection focuses on the inlet flow measurements conducted utilising 5HP probe, HW and PIV. The second subsection describes the development of stator-rotor wakes through the OGV passage. The third subsection presents the results at the outlet of the TRS with the comparison of velocity data between PIV and 7HP measurements.

3.1 Inlet measurements

The inlet plane measurements were performed by three different techniques and in three different spatial domains. Figure 4 shows the velocity field measured by 5HP and illustrates spatial domains for (i) 5HP measurements, (ii) HW measurements, and (iii) PIV measurements. The 5HP measurements were performed in a full 30-degree sector, HW measurements in a smaller sector, and the PIV measurements in a smaller region. All planar views such as Figures 4, 5 and 9 are seen from downstream the TRS.

DOI: 10.13009/EUCASS2022-6151

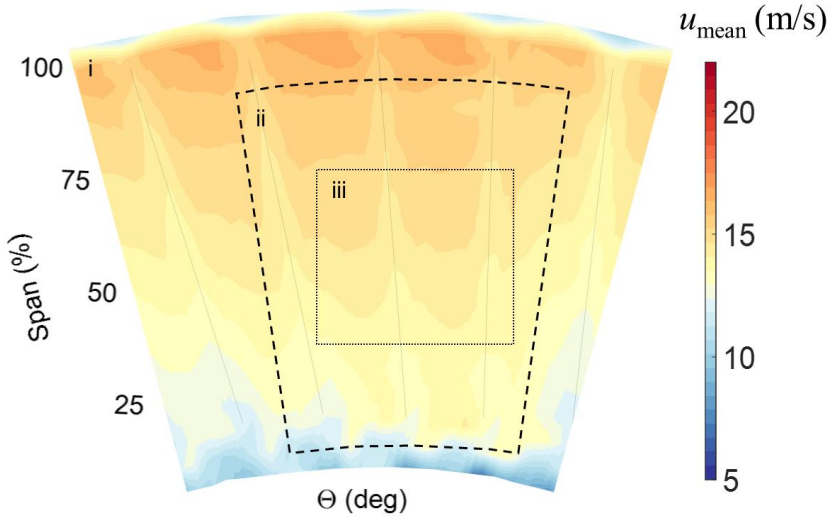

Figure 4: Mean inlet velocity field measured by 5HP probe and illustration of spatial domains for (i) 5HP measurements, (ii) HW measurements, and (iii) PIV measurements.

Three main features can be observed from the time-averaged flow field obtained with the 5HP in Figure 4. The first main feature is the periodic flow modulation due to the presence of NGV wakes, which result in low-velocity values highlighted by the grey lines and circumferential velocity modulation. The second main feature is the boundary layer on the shroud which is modulated by the corner vortices from NGVs. The third region which is worth noting is the hub endwall region. The regions of low velocity close to the hub can be attributed to the developed boundary layer over the hub surface and secondary structures from the upstream NGVs as described in [21]. The low velocity area near the hub is substantially more pronounced close to the hub compared to the shroud due to the higher swirl angles and lower total pressure. One may note the impact from the OGV on the inlet plane near the hub as an expansion of the low velocity area near the hub. The impact of the downstream OGV was also documented in [21] but at midspan. Furthermore, even though the NGVs are mounted purely radially upstream, the wakes are leaned due to the radial distribution of the NGV and inlet flow turning by the turbine.

Inlet HW measurements were performed using a downstream traversing system moving the probe at the inlet area (ii). The ensemble averaged velocity is time-dependent, and the perturbation velocity contour is plotted at a certain particular time of LPT passing.

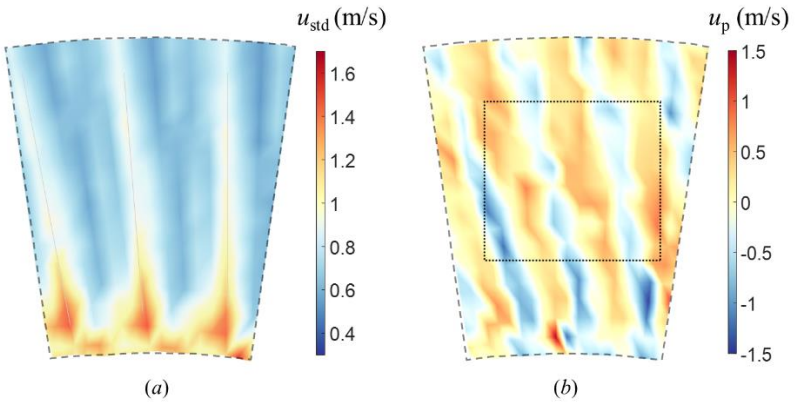

Figure 5: (*a*) Standard deviation of ensemble averaged velocity and (*b*) perturbation velocity from HW measurements at inlet plane (ii).

The standard deviation velocity contour results reveal three NGV wakes with high-velocity fluctuations that match with previously shown low-velocity regions from the 5HP in Figure 4. Furthermore, regions of increased velocity fluctuations in the wakes near the hub can be seen for all three NGV wakes within the measurement area. For the velocity perturbation contour plot, Fig. 5, *b*, the rotor wakes are represented by regions of negative perturbation velocity difference relative to the local mean velocity. A large section of the freestream in Fig. 5, *b* has a clear correlation to the passing rotor as the negative perturbations follows a continuous line according to inlet flow angles. One can also notice a non-symmetric tangential distribution of rotor wake intensity, especially at midspan where the

DOI: 10.13009/EUCASS2022-6151

velocity fluctuations of the rightmost wake are higher than the leftmost which is likely cause by the OGV interaction. A rectangle depicted with a dotted line is shown to indicate the PIV measurement domain.

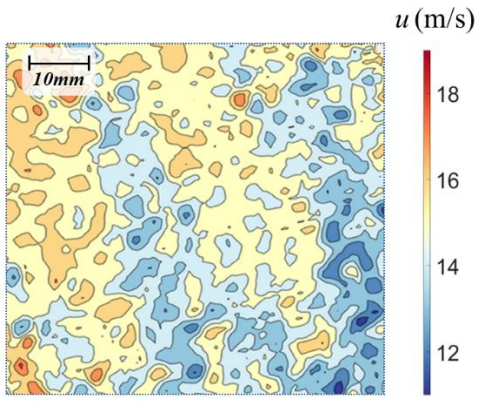

Figure 6: Instantaneous velocity field from PIV measurements at inlet plane in domain (iii).

Figure 6 shows an instantaneous velocity field obtained at the TRS inlet / LPT outlet by PIV in the domain (iii). A closer look at the PIV results reveals fundamentally crucial results on the inflow structure. The PIV results confirm the observed rotor wakes by the triggered HW perturbations in the domain (iii). Two LPT blade wake regions with a velocity deficit in the measured velocity field can be identified. As can be seen, the rotor wakes originated from the LPT and the space between them are strongly modulated by small-scale vortices approximately 5 mm in size.

3.2 Downstream development

To provide an overview of the flow development through the TRS the standard deviation of ensemble-averaged velocity and perturbation velocity at three measurement planes downstream LPT are presented in Figure 7.

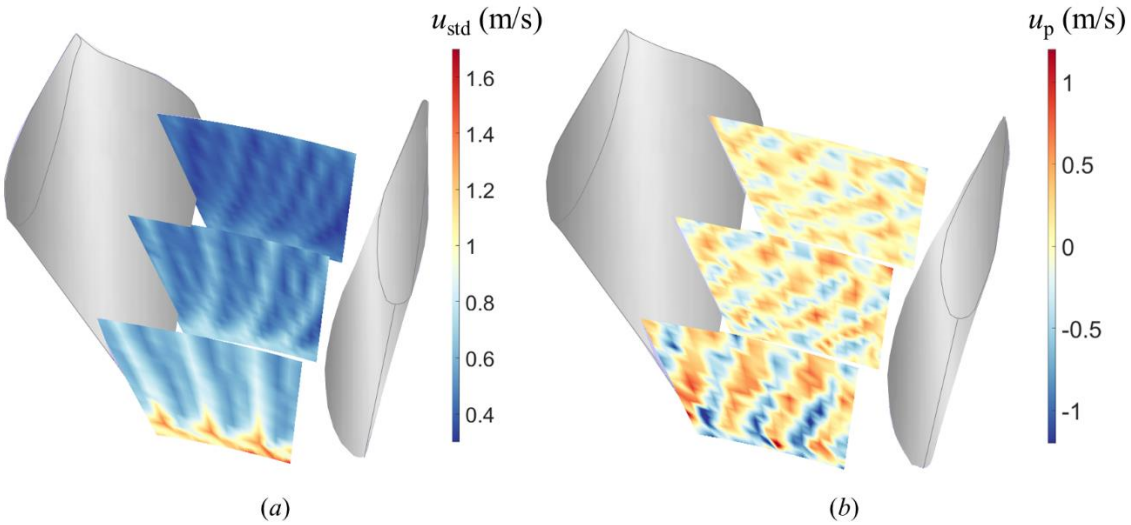

Figure 7: (*a*) The standard deviation of ensemble-averaged velocity and (*b*) perturbation velocity at three axial planes: 176, 256 and 336 mm.

The standard deviation contour plot (Fig. 7, *a*) highlights the development of the stator wakes and the perturbation velocity contour plot (Fig. 7, *b*) highlights the development of the rotor wakes at axial positions x=176, 256, 336 mm from inlet reference position. Even though the indications of the stator wakes exist in the downstream plane the velocity fluctuations decay significantly. The standard deviation is a measure of unsteadiness of velocity in the wake. Current OGVs are hub-loaded and turn the flow near the hub by 40 degrees more than near the shroud (Vikhorev et al. [13]). Therefore, the convection of the stator wakes within the volume between OGVs is characterized by bowing of the stator wakes. However, the flow past TRS is affected by the wakes of NGVs and the wakes of the

DOI: 10.13009/EUCASS2022-6151

LPT rotor. The contour plot of perturbation velocity (Fig. 7, *b*) highlights the rotor wake pattern and its development through the measurement volume. As the flow develops downstream, the rotor wakes are tilted compared to the inlet plane. In addition, the wake structure becomes more staggered due to the modulation by the periodic stator wakes, while the level of perturbation velocity decreases. The latter can be seen by looking at the time series of the ensemble-averaged and instantaneous velocity at fixed radial and tangential location in the bulk flow at three axial positions downstream LPT (Fig. 8).

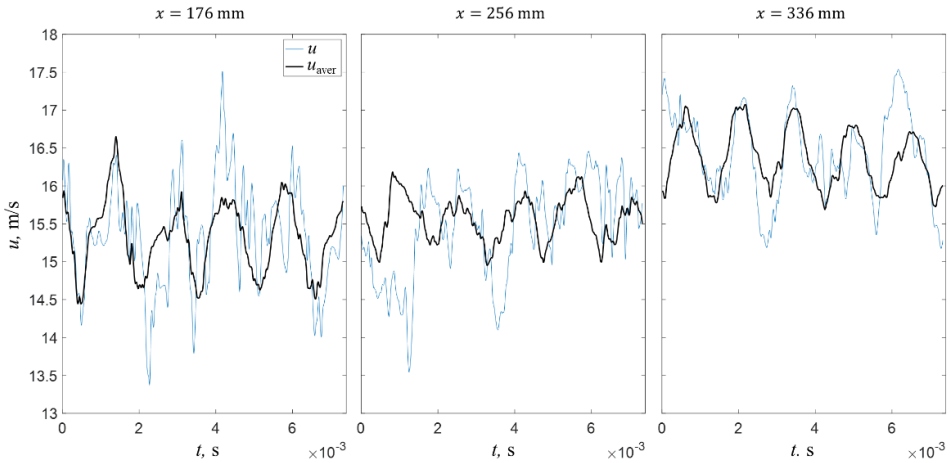

Figure 8: Instantaneous and ensemble-averaged velocity time series in the bulk flow at three axial locations: 176, 256 and 336 mm.

3.3 Outlet measurements

This section presents the velocity measurements at the outlet plane of the TRS. The outlet measurements are performed utilising 7HP and PIV technique, see Fig. 9. The mean velocity values from the 7HP are obtained at outlet 30-degree sector (i) located downstream OGV with OGV centred in the middle of the sector. The PIV measurements are obtained at outlet domain (ii) marked by a dot-dashed line in Fig 9, *a*.

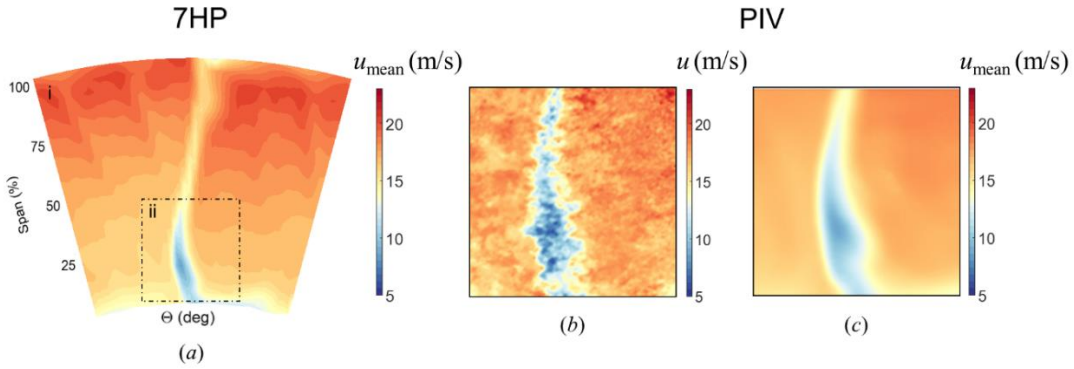

Figure 9: (*a*) Mean velocity distribution from the 7HP and PIV contours of (*b*) instantaneous and (*c*) mean velocity at the outlet plane.

As can be seen from the velocity contour plot from the 7HP (Fig. 9, *a*), the development of NGV stator wakes lead to non-uniform circumferential velocity modulation. The 7HP and PIV measurements show good agreement with the mean velocity results. Closer inspection of the instantaneous and mean velocity distributions (Figure 9, *b* and *c*) obtained from PIV measurements indicate the unsteady modulation of the wake by small-scale vortices as a result of developed OGV boundary layers.

DOI: 10.13009/EUCASS2022-6151

4. Conclusions

A detailed experimental aerodynamic study on the LPT wake interaction and development within TRS is presented. The experiments were performed at on-design condition corresponding to a Reynolds number of 235,000 and a flow coefficient of 0.622. In order to characterise the flow in TRS, different measurement techniques were applied. For the first time, the steady and time-resolved measurements of the flow within TRS were performed utilising HW and PIV experimental techniques. These investigations complement previous inlet and outlet measurements using multi-hole probes.

From the measurements it is clear that unsteady and steady flow modulation is the strongest at the inlet of the TRS, as expected, with propagation through the TRS. The comparison of the inlet velocity contours between 5HP and HW shows good agreement. The instantaneous velocity contour from PIV measurements complements the HW results and indicates the rotor wakes modulated by small-scale vortices. As the flow proceeds through the TRS, the fluctuation levels are decreased and show a more uniform behavior. Moreover, the rotor and stator wakes are leaning because of the gradient in swirl angle and their interaction leads to a staggered pattern of the rotor wakes. The comparison of outlet velocity contours between PIV and 7HP measurements shows good agreement. It is shown that outlet velocity distribution is weakly affected by the rotor and stator wakes, resulting in weak circumferential modulation. Besides giving a detailed insight into the wake development of the TRS, these measurements will serve as a useful database for CFD validation and future TRS designs.

5. Acknowledgements

The authors would like to gratefully acknowledge financial support from the NFFP (Nationella flygtekniska forskningsprogrammet) and the EU-Commission. This project has received funding from the Clean Sky 2 Joint Undertaking under the European Union's Horizon 2020 Research and Innovation Program under grant agreement No 821398. Chalmers Laboratory of Fluids and Thermal Sciences is acknowledged for hosting the facility and the measurement equipment.

Nomenclature

H	channel height at inlet, m
Re	Reynolds number, U_xH/ν
V	blade velocity, m/s
U_x	axial flow velocity, m/s
u	instantaneous streamwise velocity, m/s
u_{aver}	averaged velocity, m/s
u_{mean}	mean velocity, m/s
u_p	perturbation velocity, m/s
u_{std}	standard deviation of velocity, m/s
x	axial coordinate, m
φ	flow coefficient, U_x/V
θ	angular coordinate, deg

Abbreviations

5HP	5-hole probe
7HP	7-hole probe
GTF	geared turbofan engine
HW	hot-wire anemometry
LPT	low pressure turbine
NGV	nozzle guide vane
OGV	outlet guide vane
PIV	particle image velocimetry
TRS	turbine rear structure

DOI: 10.13009/EUCASS2022-6151

References

[1] Sharma, O.P., Butler, T.L., Joslyn, H.D., and Dring, R.P. 1985. Three-Dimensional Unsteady Flow in an Axial Flow Turbine. *AIAA Journal of Propulsion*. 1:29-38.

[2] Lefcort, M.D. 1965. An Investigation into Unsteady Blade Forces in Turbomachines. *ASME Journal of Engineering for Power*. 20:345–354.

[3] Raj, R., and Lakshminarayana, B. 1973. Characteristics of the wake behind a cascade of airfoils. *Journal of Fluid Mechanics*. 61(4):707–730

[4] Sieverding, C.H. 1985. Recent progress in the understanding of basic aspects of secondary flows in turbine blade passages. *Journal of Engineering for Gas Turbines and Power*. 107:248–257

[5] Langston, L., Nice, M., and Hooper, R. 1977. Three-Dimensional Flow Within a Turbine Cascade Passage. *Journal of Engineering for Power*. 99:21–28

[6] Langston, L. 1980. Crossflows in a Turbine Cascade Passage. *Journal of Engineering for Power*. 102:866–874

[7] Yamamoto, A. 1987. Production and Development of Secondary Flows and Losses in Two Types of Straight Turbine Cascades: Part 1—A Stator Case. *ASME Journal of Turbomachinery*. 109(2):186–193.

[8] Yamamoto, A. 1987. Production and Development of Secondary Flows and Losses in Two Types of Straight Turbine Cascades: Part 2—A Rotor Case. *ASME Journal of Turbomachinery*. 109(2):194–200.

[9] Langston, L. 2006. Secondary flows in axial turbines—A review. Annals of the New York Academy of Science.

[10] Mayle, R.E. The Role of Laminar-Turbulent Transition in Gas Turbine Engines. In: *ASME 1991 International Gas Turbine and Aeroengine Congress and Exposition*. *Volume 5: Manufacturing Materials and Metallurgy; Ceramics; Structures and Dynamics; Controls, Diagnostics and Instrumentation; Education; IGTI Scholar Award; General*. Paper No: 91-GT-261.

[11] Schroder, T. 1989. Measurements with Hot-Film Probes and Surface Mounted Hot-Film Gauges in a Multistage Low Pressure Turbine. In: *European Propulsion Forum*. 15.1–15.27.

[12] Hodson, H.P. 1985. Measurements of Wake Generated Unsteadiness in the Rotor Passages of Axial Flow Turbines. *ASME Journal of Engineering for Gas Turbines and Power*. 107:337–344.

[13] Vikhorev, V., Chernoray, V., Thulin, O., Deshpande, S., and Larsson, J. 2021. Detailed experimental study of the flow in a turbine rear structure at engine realistic flow conditions. *ASME Journal of Turbomachinery*.143(9). Paper No: TURBO-20-1372.

[14] Jonsson, I., Chernoray, V., and Rojo, B. 2018. Surface Roughness Impact on Secondary Flow and Losses in a Turbine Exhaust Casing. In: ASME Turbo Expo 2018, Paper No: GT2018- 75541.

[15] Jonsson, I., Chernoray, V., and Dhanasegaran, R. 2020. Infrared Thermography Investigation of Heat Transfer on Outlet Guide Vanes in a Turbine Rear Structure. *International Journal of Turbomachinery, Propulsion and Power*. 5(3): 23-35.

[16] Jonsson, I., Deshpande, S., Chernoray, V., Thulin, O., and Larsson, J. 2021. Experimental and Numerical Study of Laminar-Turbulent Transition on a Low-Pressure Turbine Outlet Guide Vane. *ASME Journal of Turbomachinery*. 143(10). Paper No: TURBO-20-1415.

[17] Deshpande, S., Jonsson, I., and Chernoray, V. 2019. Effect of Surface Roughness on Aerodynamic Performance of Turbine Rear Structure. In: ASME Turbo Expo 2019. Paper No: GT2019-90472.

[18] Vikhorev, V., and Chernoray, V. 2021. Experimental Flow Analysis in a Modern Turbine Rear Structure with 3D Polygonal Shroud under Realistic Flow Conditions. In: 14th European Turbomachinery Conference on Turbomachinery Fluid Dynamics and Thermodynamics, Virtual conference. Paper No: ETC2021-539.

[19] Vikhorev V., Nylander P., Chernoray V., Larsson J., and Thulin, O. 2022. Experimental and Numerical Flow Analysis of an Engine-Realistic State-of-the-Art Turbine Rear Structure. *Journal of Engineering for Gas Turbines and Power*. 144(7). Paper No: GTP-22-1022.

[20] Rojo, B., Kristmundsson, D., Chernoray, V., Arroyo, C., and Larsson, J. 2015. Facility for Investigating the Flow in a Low Pressure Turbine Exit Structure. In: 11th European Conference on Turbomachinery Fluid Dynamics and Thermodynamics, ETC 2015. Paper No: ETC2015-235

[21] Rojo, B. 2017. Aerothermal Experimental Investigation of LPT-OGVs. PhD Thesis, Chalmers University of Technology, Gothenburg, Sweden.